



# Assessing the Stability of Ships under the Effect of Realistic Wave Groups

Panayiotis A. Anastopoulos, *Department of Naval Architecture and Marine Engineering, National  
Technical University of Athens, Greece, [panasto@central.ntua.gr](mailto:panasto@central.ntua.gr)*

Kostas J. Spyrou, *Department of Naval Architecture and Marine Engineering, National Technical  
University of Athens, Greece, [k.spyrou@central.ntua.gr](mailto:k.spyrou@central.ntua.gr)*

## ABSTRACT

Ship propensity for stability failure in random beam seas is addressed. A novel method based on the systematic construction of realistic wave groups is proposed. Derived waveforms are sequences of varying heights and periods with high probability of occurrence. To demonstrate the approach, stability analysis is performed on a modern container vessel using an uncoupled equation of roll motion. The effects of height and period variations on the system's transient response and on the integrity of its safe basin are discussed against the context of a "regular sea" investigation.

**Keywords:** *irregular seas, wave groups, transient capsizing, safe basin erosion, integrity curves, Karhunen-Loève theorem*

## 1. INTRODUCTION

The study of large amplitude ship motions in a stochastic sea is one of the most challenging computational tasks in naval architecture. On the one hand, advanced methods of nonlinear dynamics are indispensable for yielding insights into the mechanisms of capsizing. At the same time, however, such methods have not been so practical for providing estimates of capsizing tendency, especially when employing computationally expensive numerical techniques. This is compounded by the fact that, for quantitative accuracy in dynamic stability predictions, detailed hydrodynamic modelling is highly desirable. For rare phenomena like capsizing, the efficiency of long-time simulations on heavy models is disputed since most of the time is idly expended on simulating innocuous ship-wave encounters. This has motivated the development of a number of techniques for directly extracting those time intervals when hazardous wave episodes occur.

A relevant phenomenon, often observed in wind-generated seas, is wave grouping. Wave groups are sequences of high waves with periods varying within a potentially small range (Masson & Chandler, 1993, Ochi, 1998). Notably, the occurrence of dangerous wave group events, leading to motion augmentation, does not necessarily imply exceptionally high waves. Resonant phenomena, often "felt" in the first few cycles of wave group excitation, are crucial for the integrity of a marine system. The manifestation of ship instability under the effect of wave groups was the objective of three recent studies, reviewed, in brief, next.

Reaping the benefits coming from the separation of dynamics from randomness, the "critical wave groups" approach disassembles the problem in a deterministic and a probabilistic part (Themelis & Spyrou, 2007). In the former, critical combinations of heights, periods and run lengths, related to regular wave groups that incur unacceptably large dynamic



response, are identified. The critical, in terms of ship stability, waveforms represent basically thresholds, defined by regular wave trains. Statistical analysis of the seaway is included in the probabilistic part of the approach. The propensity for ship stability failure is quantified by calculating the probability of encountering any train higher than the determined critical threshold.

A statistical approach for the prediction of extreme parametric roll responses was presented in the study of Kim & Troesch (2013). The method is based on the assumption that the fluctuation of instantaneous GM is a Gaussian random process. The “Design Loads Generator” was employed to generate an ensemble of irregular wave groups, associated with the extreme value distribution of a surrogate process, representing time-varying metacentric height groups (Kim, 2012). The derived wave trains, realized as a lower bound of the “true” excitation, were, eventually, utilized as input to a high fidelity hydrodynamic system for simulating the actual nonlinear response of a C11 containership.

Malara et al. (2014) proposed an approach for the estimation of the maximum roll angle, induced by spectrum compatible wave group excitation. Representation of the load process in the vicinity of an exceptionally high wave was formulated within the context of the “Quasi-Determinism” theory (Boccotti, 2000). The approach is asymptotically valid in the limit of infinitely high waves and its use is possibly suitable for heights at least twice the significant wave height of the considered sea state (Boccotti, 2000).

In the following section, a new, spectrum compatible, method of wave group loads is proposed. The method expands upon Themelis & Spyrou (2007) on the one hand, by considering realistic wave group profiles; and on Malara et al. (2014) by removing the “extreme waves” assumption imposed by the theory of Quasi-Determinism. The objective is an in-depth investigation of the effects of short

duration irregular seaways on the transient response and engineering integrity of a modern container vessel.

## 2. MODELLING OF WAVE GROUP LOADS

### 9.1 Stochastic treatment of wave successions

The assumption of height sequences which fulfil the Markov property has been employed with remarkable success in a number of studies for the derivation of wave groupiness measures (Kimura, 1980, Battjes & van Vledder, 1984, Longuet-Higgins, 1984). On the other hand, the application of straightforward spectral techniques, targeting the statistical elaboration of wave period groupings, is full of inherent limitations.

Recently, an extended Markov-chain model, allowing for cross-correlations between successive heights and periods, was proposed (Anastopoulos et al., 2014). A computational method, based on envelope analysis in conjunction with the theory of copula distributions, produced explicit formulas for the transition probabilities of the process. The joint expectations of consecutive heights  $h_i$  and periods  $t_i$  were expressed by the following set of coupled equations:

$$h_i = \int_0^{\infty} h_i f_{H_i|H_{i-1}, T_{i-1}}(h_i|h_{i-1}, t_{i-1}) dh_i \quad (1a)$$

$$t_i = \int_0^{\infty} t_i f_{T_i|H_{i-1}, T_{i-1}}(t_i|h_{i-1}, t_{i-1}) dt_i \quad (1b)$$

where  $H$  and  $T$  are the height and period random variables at time step  $i$ , with state variables  $h$  and  $t$ , respectively. The “most expected” wave sequence can iteratively be constructed using equations (1a)-(1b). The whole waveform becomes explicitly dependent

on the wave occupying the centre of the group if the key characteristics of the highest wave are selected as initial conditions for the iteration process.

## 2.1 Estimating transition kernels via Monte Carlo simulations

Comprehensive description of the analysis associated with the theoretical estimation of the transition kernels, given by equations (1a) and (1b), can be found in Anastopoulos et al. (2014). In this study, a JONSWAP spectrum (Hasselmann et al., 1973), with peak period  $T_p = 13.6s$  and significant wave height  $H_s = 10m$ , was considered in order to simulate time series of water surface elevation. The main idea is to arrange the generated data in the following vector sets and proceed to regression analysis.

$$\mathbf{A} = \begin{bmatrix} h_i \\ h_{i-1} \\ t_{i-1} \end{bmatrix}, \quad \mathbf{B} = \begin{bmatrix} t_i \\ h_{i-1} \\ t_{i-1} \end{bmatrix} \quad (2)$$

Then, the transition mechanisms can be expressed through a best-model-fit method. Figure 1 explains the concept of a “correlation surface”, which fits data of vector  $\mathbf{A}$ . In the same figure, the  $(h_i-t_i)$  plane corresponds to the total population of joint height-period realizations. The smoothened bivariate height and joint height-period distributions for successive waves are also provided.

## 2.2 The Karhunen-Loève representation

The Karhunen-Loève theorem is employed in order to construct continuous-time analogues of wave sequences, related to the predictions of the Markov-chain model described before (Karhunen, 1947, Loève, 1978). The main advantage of the specific approach over the traditional Fourier series representation is that it ensures the minimum total mean-square error resulting out of its truncation. In other words,

all the information provided by the auto-covariance function of the original process, can efficiently be integrated within the few waves of a group sequence. The theorem states that the water surface displacement  $\eta$  admits the following decomposition:

$$\eta(x,t) = \sum_{n=0}^{\infty} a_n f_n(x,t), \quad -T < t < T \quad (3)$$

In the case of a Gaussian random process, the coefficients,  $a_n$  ( $n = 0,1,\dots$ ), are random independent variables. An efficient computational procedure for the basis functions  $f_n$  is described in Sclavounos (2012).

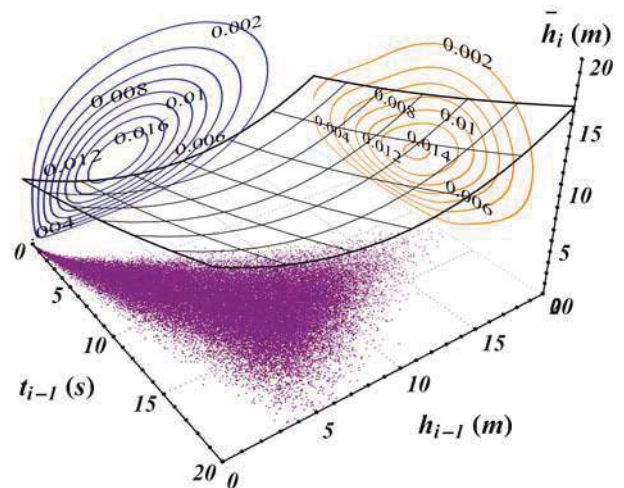


Figure 1: Correlation surface for the prediction of the “most expected” wave heights.

Spectrum compatible wave loads can directly be constructed if appropriate geometric constraints are imposed on equation (3). The key is to formulate a well-defined interpolation problem for the values of water surface displacement at time instants when crests, troughs and zero-crossings occur. To this end, the truncation of the series expansion (3) should be explicitly dependent on the number of waves  $j$  participating in the group formation. In this case, the space-time expansion of the original process  $\eta$  is reformulated as:



$$\eta(x,t) = \sum_{n=0}^{6j} a_n f_n(x,t), \quad -T < t < T \quad (4)$$

The Markov-chain/Karhunen-Loève (MC-KL) model was employed to generate the family of irregular wave groups, shown in Figure 2. The derived waveforms are comprised of  $j = 5$  waves and correspond to the same central wave period  $T_c$ . The root-mean-square value ( $H_{rms}$ ) of the simulated sea state heights was the assumed threshold that individual wave heights should exceed. As demonstrated, groups of different durations arise when changing the value of the central wave height  $H_c$ . Furthermore, the convergence rate of the approach is tested in Figure 3. The vertical axis denotes the absolute relative error with respect to the estimation of the spectral variance; and the horizontal axis, the corresponding number of stochastic components kept in equation (3). Considering a run length of  $j = 5$  waves would result in a small truncation error of approximately 2%.

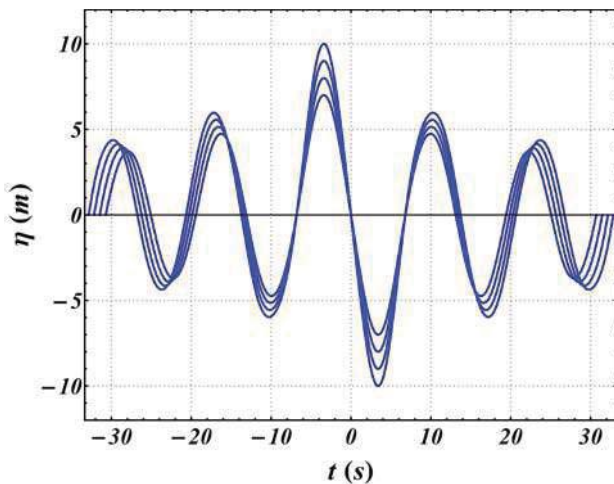


Figure 2: Wave groups of increasing  $H_c = 14\text{m}$ ,  $16\text{m}$ ,  $18\text{m}$  and  $20\text{m}$ .  $T_c = T_p$ .

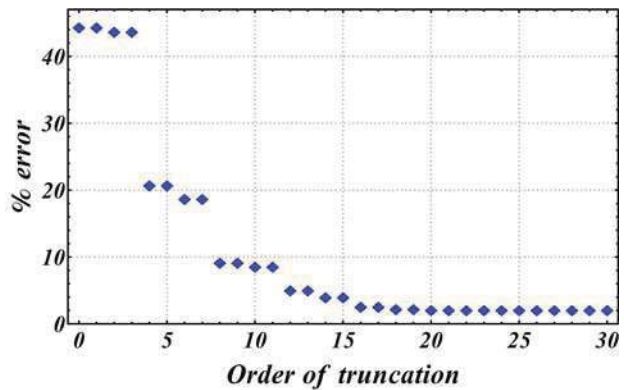


Figure 3: Error in spectral variance for various truncation orders.

### 2.3 Roll motion in long-crested irregular wave groups

A 4800 TEU panamax containership was selected for a preliminary application of the method. The main particulars and the considered loading condition are shown in Table 1. No information about the existence of bilge keels was provided; thus, the bare hull of the ship, shown in Figure 4, was only considered.

Table1: Ship main particulars

Displacement ( $\Delta$ )	68199	Tons
Length between perpendiculars ( $L_{BP}$ )	238.35	m
Breadth ( $B$ )	37.30	m
Draught ( $T$ )	11.52	m
Depth ( $D$ )	19.60	m
Service speed ( $V_s$ )	21	kn
Metacentric height ( $GM$ )	2.85	m
Natural period ( $T_0$ )	15.25	s



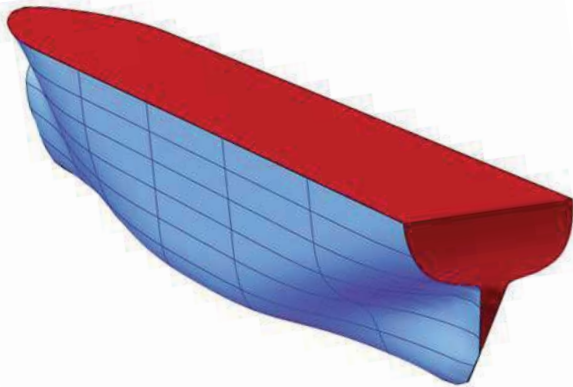


Figure 4: The hull of the containership modelled with *Mathematica*®.

In the presence of long incident waves, ship motion is studied under the Froude-Krylov assumption. In this case, the following uncoupled equation, written in terms of the relative roll angle  $\varphi$ , is employed:

$$(I_{44} + A_{44})\ddot{\varphi} + D(\dot{\varphi}) + \Delta GZ(\varphi) = M_{wave}(t) \quad (5)$$

where  $I_{44}$  and  $A_{44}$  are the roll moment of inertia and the added moment, respectively. Customary quadratic damping moment  $D$  is assumed:

$$D(\dot{\varphi}) = B_1\dot{\varphi} + B_2\dot{\varphi}|\dot{\varphi}| \quad (6)$$

The damping coefficients were calculated according to the hydrodynamic component moment analysis, described in Ikeda et al. (1978). To the  $GZ$ -curve was fitted a 9th degree polynomial. The wave induced moment was modelled as (Wright & Marshfield, 1980):

$$M_{wave}(t) = -I_{44}\ddot{\alpha}(t) \quad (7)$$

with  $\alpha$  being the instantaneous wave slope at the middle of the ship.

### 3. TRANSIENT CAPSIZE DIAGRAMS

The “transient capsizing diagram” is a plot of wave period against the steepness ratio associated with critical, from ship dynamics perspective, roll angles (Rainey & Thompson, 1991). Ship motion in real seas is inherently transient and the use of steady-state analysis can be only indicative (Spyrou & Thompson, 2000). Below we shall extend the idea of the transient capsizing using the MC-KL model in order to identify thresholds of unsafe behaviour under the “most expected” wave group loads. This can offer a rational treatment to problem of quantifying low-probability wave encounters.

Calculating transient capsizing diagrams in the case of regular wave groups is a straightforward procedure, commonly advocated in the literature. On the other hand, analysis of the system’s transient response in irregular seas can turn into a complicated task, mostly due to the lack of necessary definitions. The appropriate selection of wave group characteristics, to be labelled on the stability diagram, is the greatest concern in the specific approach. In order to provide satisfactory answers to this issue, separation of height from period variations was attempted. Transient capsizing diagrams were eventually calculated for the three cases shown in Table 2.

Table 2: Wave group case studies

Case	Description
01	<i>Regular wave groups</i>
02	<i>Regular wave groups with varying heights</i>
03	<i>MC-KL wave groups</i>

The construction algorithm of wave sequences related to Case 02 is based on simple manipulations of the MC-KL model. Firstly, joint height-period successions were calculated according to the original formulation of the method. Cross-correlations between consecutive heights and periods were fully



considered. In the end, however, the predicted periods were discarded and the derived height sequences were associated with constant periods. The Karhunen-Loève theorem was applied again to construct continuous counterparts.

In all three cases of Table 2 the produced wave groups were comprised of  $j = 5$  individual waves with heights greater than  $H_{rms}$ . Moreover, without loss of generality, zero initial conditions at the moment of encounter were assumed. According to the Weather Criterion ship capsizes was considered the exceedance of the down-flooding angle  $\varphi_f = 40$ degrees.

### 3.1 The effect of height variations

In Figure 5 the transient capsizes diagrams of Cases 01 and 02 are superimposed. The “mean wave steepness” curve, denoted by  $H_m/\lambda$ , was calculated from the average wave height  $H_m$  of groupings derived for Case 02. The steepness ratio of the respective highest wave is given by the  $H_c/\lambda$  - curve. The horizontal axis is the non-dimensional wave period  $T$  with respect to the ship natural period  $T_0$ .

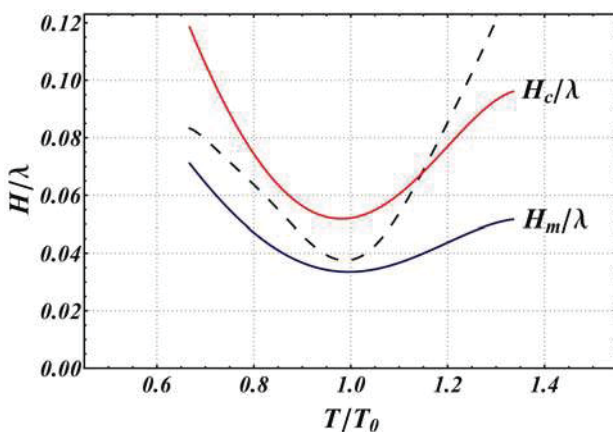


Figure 5: Transient capsizes diagrams for Cases 01 (dashed line) and 02 (solid lines).

Figure 5 reveals the existence of three regions with qualitatively different stability features. In region A ( $T/T_0 \leq 0.85$ ) the critical steepness

ratio of the regular wave trains was found very close to that of the maximum wave, calculated in Case 02. Rapid exceedance of  $\varphi_f$  was encountered, in both cases, within the first three wave cycles. In region B ( $0.85 < T/T_0 \leq 1.10$ ), which is the region of resonant response, the two methods are totally equivalent. Since  $j$  was constantly fixed, the produced wave groups were of exactly the same duration. Moreover, height variations were found to have little influence on the performance of the vessel considering that the mean critical steepness  $H_m/\lambda$  was approximately the same for both methods. Stability failure was experienced after the third wave cycle. Finally, in region C ( $T/T_0 > 1.10$ ) the two methods exhibit substantial discrepancies. The key finding is that roll motion is build-up during the developing stage of non-periodic wave groups. The position of the highest wave plays a crucial role for the manifestation of instability, leading to moderate critical steepness predictions.

### 3.2 The effects of period variations

In the same spirit, the transient capsizes diagrams of Cases 01 and 03 are shown in Figure 6. The period of the highest wave of a single run is  $T_c$ . In Figure 7 critical wave groups of Case 03 are represented in terms of the average period ( $T_{avg}$ ) and shortest period ( $T_{min}$ ) in a non-dimensional form with respect to  $T_c$ .

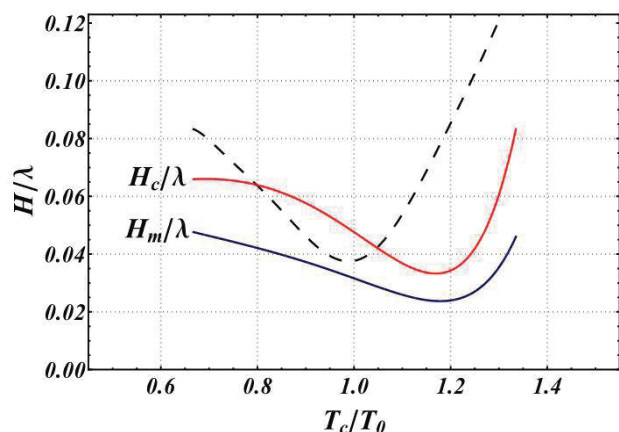


Figure 6: Transient capsizes diagram for Cases 01 (dashed line) and 03 (solid lines).

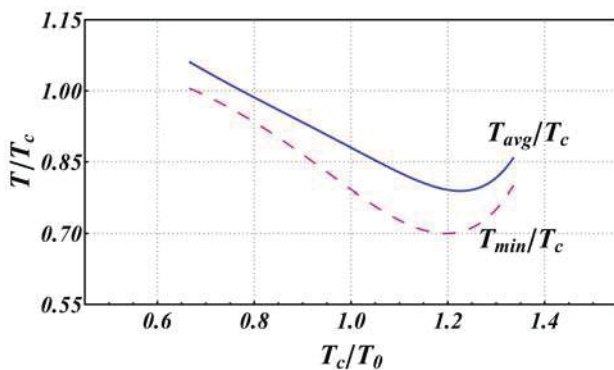


Figure 7: Period variations for Case 03; solid line:  $T_{avg}/T_c$ , dashed line:  $T_{min}/T_c$ .

Figure 6 indicates that modelling of realistic period successions results in a wider instability area, shifted to the region of long waves. In a typical MC-KL wave group the highest wave is surrounded by two waves with only slightly different periods. This fact, also reported in the experimental study of Su (1986), implies an “almost regular” waveform in the vicinity of the high central wave. In Figure 7 such phenomena are mostly associated with region A. However, motion augmentation is still possible in regions B and C if estimated periods vary within a sufficiently small range.

In Figure 8 short time histories of simulated roll motion are displayed. Ship responses that exceed plot boundaries are related to capsizing events, included in Figures 5 and 6. Dashed, thin and thick lines denote Cases 01, 02 and 03, respectively. The upper panel is associated with region A, where quick violation of the capsizing criterion is experienced in all case studies. In region B resonant phenomena dominate resulting in dangerous build-up of roll motion (middle panel). Finally, in region C, exceptionally high regular wave trains led to immediate capsizing (bottom panel). On the other hand, Cases 02 and 03 produced progressively increasing roll amplitudes.

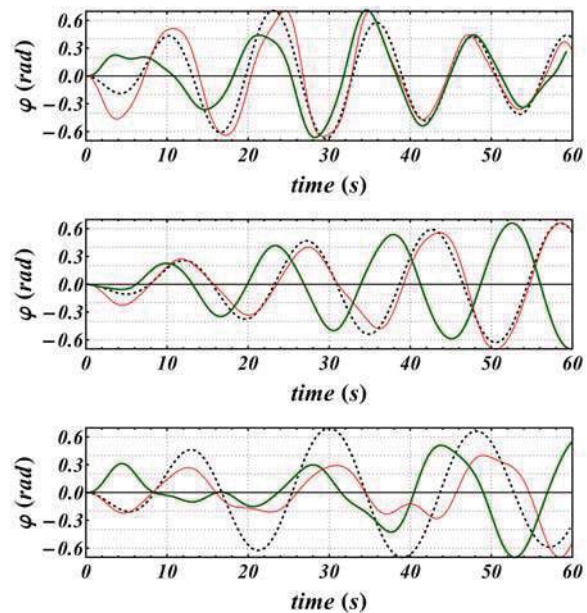


Figure 8: Roll response time-histories; upper panel:  $T_c/T_0 = 0.789$ , middle panel:  $T_c/T_0 = 1.049$ , lower panel:  $T_c/T_0 = 1.246$ .

#### 4. SAFE BASIN EROSION AND INTEGRITY CURVES

In this section the non-linear response of the system is investigated up to the limiting angle of vanishing stability  $\varphi_v = 66$ degrees. Basins of attraction are constructed after repeated simulations of ship motion with different initial conditions. The short duration of wave group excitation allows for a considerable reduction of the computational burden. In the study of Thompson (1989) rapid erosion and stratification of the safe basin was observed to take place under small variations of the wave parameters. The same logic is applied below using the MC-KL approach.

In Figure 9 the “integrity curves” of the vessel are illustrated. The probability of capsizing is quantified by the ratio of the actual safe basin area over the estimated area in free decay. The horizontal axis is the non-dimensional central wave height  $H_c$  with respect to Airy breaking limit  $H_0$ . Analysis was performed for a fixed central wave period  $T_c =$



$T_p$ . Rapid loss of engineering integrity is observed when modelling successions of realistic wave periods.

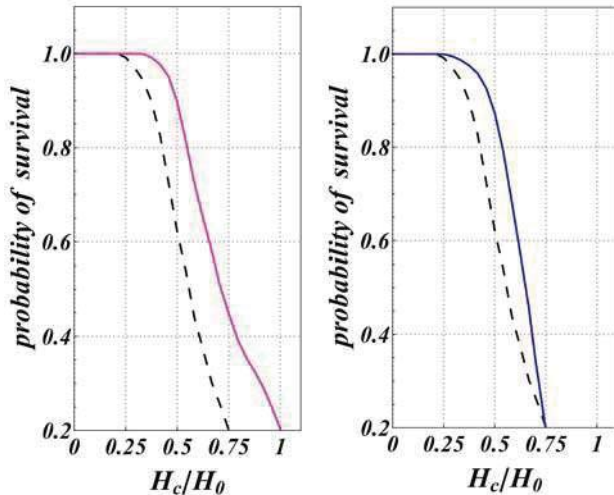


Figure 9: Integrity curves; left panel: Cases 01 (dashed line) & 02 (solid line); right panel: Cases 01 (dashed line) & 03 (solid line).

Basins of attraction, indicating 10% and 40% loss of the originally safe area appear in Figure 10. The graphs correspond to a 400x400 grid of initial conditions. Black colour implies initial conditions that led to quick capsizing, practically within the first wave cycle. Purple and blue regions indicate capsizing during the second and third wave cycles, respectively. Safe regions remained uncoloured. In the case of regular group excitation, striations arise close to the basin boundary. At later stages of the erosion process these striations expand rapidly to the internal of the initially safe basin. On the other hand, for Cases 02 and 03 the basins start to erode “from within”. In most cases capsizing is experienced when encountering the highest wave of the train.

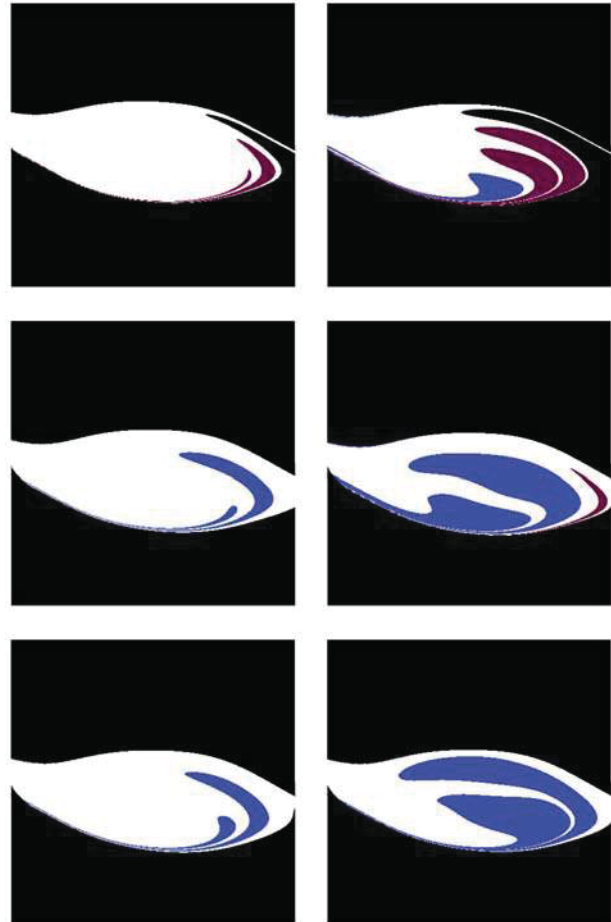


Figure 10: Transient basin erosion. Left column: 10% integrity loss; right column: 40% integrity loss; from top to bottom: Cases 01, 02, 03.

## 5. CONCLUSIONS

A new model for the systematic construction of spectrum-compatible wave group loads was presented. The effects of wave grouping phenomena on the performance of a modern containership were investigated. Stability analysis was performed in terms of transient capsizing diagrams. The idea was to simulate wave induced moments with high probability of occurrence and study separately the effects of height from period variations within the group formations. The results indicate that realistic wave groups yield a wide instability region, yet shifted with respect to the regular case. In some cases, lower capsizing





thresholds were defined by wave successions of gradually increasing heights rather than common regular trains. Finally, the concept of quantifying safe operational conditions through integrity curves was discussed. The conclusion is that the sudden erosion of the safe basin caused by irregular wave group excitation is a qualitatively different process from the typical regular approach.

## 6. ACKNOWLEDGMENTS

This work has been supported by the Greek General Secretariat of Research and Technology under the General Program "ARISTEIA I" (contract reference number GSRT-252).

## 7. REFERENCES

- Anastopoulos, P.A., Spyrou, K.J., Bassler, C.C., and Belenky, V., 2014, "Towards an improved critical wave groups method for the assessment of large ship motions in irregular seas", Proceedings of the 7th International Computational Stochastic Mechanics Conference, Santorini, Greece (to be published).
- Battjes, J.A., and van Vledder, G.P., 1984, "Verification of Kimura's theory for wave group statistics", Proceedings of the 19th International Coastal Engineering Conference, ASCE, Houston, TX, pp. 642-648.
- Boccotti, P., 2000, "Wave Mechanics for Ocean Engineering", Elsevier, Oxford, England, ISBN: 978-0-444-50380-0.
- Hasselmann, K. et al, 1973, "Measurements of wind-wave growth and swell decay during the Joint North Sea Wave Project (JONSWAP)", Deutschen Hydrographischen Zeitschrift, A.12, pp. 1-95.
- Ikeda, Y., Himeno, Y., and Tanaka, N., 1978, "A prediction method for ship roll damping", Report No. 00405 of Department of Naval Architecture, University of Osaka Prefecture.
- Karhunen, K., 1947, "Über lineare Methoden in der Wahrscheinlichkeitsrechnung", Annales, Academiae Scientiarum Fennicae. Ser. A. I. Math.-Phys., Vol. 37, pp. 1-79.
- Kim, D-H., 2012, "Design loads generator: Estimation of extreme environmental loadings for ship and offshore applications", PhD thesis, The University of Michigan.
- Kim, D-H., and Troesch, A.W., 2013, "Statistical estimation of extreme roll response in short crested irregular head seas", SNAME Transactions.
- Kimura, A., 1980, "Statistical properties of random wave groups", Proceedings of the 17th International Coastal Engineering Conference, ASCE, Sydney, Australia, pp. 2955-2973.
- Loève, M., 1978, "Probability theory", Vol. II, 4th ed., Graduate Texts in Mathematics, Springer-Verlag, London, England, ISBN: 0-387-90262-7.
- Longuet-Higgins, M.S., 1984, "Statistical properties of wave groups in a random sea state", Philosophical Transactions of the Royal Society of London A, Vol. 312(1521), pp. 219-250.
- Malara, G., Spanos, P.D., and Arena, F., 2014, "Maximum roll angle estimation of a ship in confused sea waves via a quasi-deterministic approach", Elsevier Probabilistic Engineering Mechanics, Vol. 35, pp. 75-81.
- Masson, D., and Chandler, P., 1993, "Wave groups: A closer look at spectral methods", Elsevier Coastal Engineering, Vol. 20(3-4), pp. 249-275.



- Ochi, M., 1998, "Ocean Waves: The Stochastic Approach", Cambridge University Press, Cambridge, England, ISBN: 978-0-521-01767-1.
- Rainey, R.C.T., and Thompson J.M.T., 1991, "The transient capsize diagram – a new method of quantifying stability in waves", Journal of Ship Research, Vol. 35(1), pp. 58-62.
- Sclavounos, P.D., 2012, "Karhunen-Loève representation of stochastic ocean waves", Proceedings of Royal Society of London A, Vol. 468(2145), pp. 2574-2594.
- Spyrou, K.J., and Thompson, J.M.T., 2000, "The nonlinear dynamics of ship motions: a field overview and some recent developments", Philosophical Transactions of the Royal Society A, Vol. 358 (1771), pp. 1735-1760.
- Su, M.Y., 1986, "Extreme wave group in storm seas near coastal water", Proceedings of the 20th International Coastal Engineering Conference, ASCE, Taipei, Taiwan, pp. 767-779.
- Themelis, N., and Spyrou, K.J., 2007, "Probabilistic Assessment of Ship Stability", SNAME Transactions, Vol. 115, pp. 181-206.
- Thompson, J.M.T., 1989, "Chaotic phenomena triggering the escape from a potential well", Proceedings of Royal Society of London A, Vol. 421(1861), pp. 195-225.
- Wright, J.H.G., and Marshfield, W.B., 1980, "Ship roll response and capsize behaviour in beam seas", RINA Transactions, Vol. 122, pp. 129-148.